Microwave modulation of terahertz quantum cascade lasers : a transmission-line approach

Wilfried Maineult, Lu Ding, Pierre Gellie, Pascal Filloux, Carlo Sirtori, Stefano Barbieri, Tahsin Akalin, Jean-Francois Lampin, Isabelle Sagnes, Harvey E. Beere, et al.

Microwave modulation of terahertz quantum cascade lasers: a transmission-line approach

Cite as: Appl. Phys. Lett. **96**, 021108 (2010); https://doi.org/10.1063/1.3284518
Submitted: 19 August 2009 • Accepted: 08 December 2009 • Published Online: 14 January 2010

W. Maineult, L. Ding, P. Gellie, et al.

Microwave modulation of terahertz quantum cascade lasers: a transmission-line approach

W. Maineult,[1] L. Ding,[1] P. Gellie,[1] P. Filloux,[1] C. Sirtori,[1] S. Barbieri,[1,a)] T. Akalin,[2] J.-F. Lampin,[2] I. Sagnes,[3] H. E. Beere,[4] and D. A. Ritchie[4]
[1]*Laboratoire Matériaux et Phénomènes Quantiques (MPQ), UMR CNRS 7162, Université Paris 7, 10, rue A. Domont et L. Duquet, 75205 Paris, France*
[2]*Institut d'Electronique de Microélectronique et de Nanotechnologie (IEMN), UMR CNRS 8520, Université de Lille 1, Avenue Poincaré B.P. 60069, 59652 Villeneuve d'Ascq, France*
[3]*Laboratoire LPN, Route de Nozay, 91460 Marcoussis, France*
[4]*Cavendish Laboratory, University of Cambridge, J. J. Thomson Avenue, Cambridge CB3 0HE, United Kingdom*

(Received 19 August 2009; accepted 8 December 2009; published online 14 January 2010)

We report on microwave impedance measurements of metal-metal ridge-waveguide terahertz quantum cascade lasers. Experimental data, recorded at 4 K in the 100 MHz–55 GHz range, are well reproduced by distributed-parameter transmission-line simulations, showing that the modulation cutoff is limited by the propagation losses that increase for higher microwave frequencies, yielding a 3 dB modulation bandwidth of ~70 GHz for a 1 mm-long ridge. By using a shunt-stub matching we demonstrate amplitude modulation of a 2.3 THz QCL up to 24 GHz. © *2010 American Institute of Physics*. [doi:10.1063/1.3284518]

The modulation of terahertz (THz) radiation has recently attracted a great deal of attention.[1–4] In this context THz quantum cascade lasers (QCLs) are promising devices, thanks to their short nonradiative- and stimulated-lifetimes in the picosecond range, potentially giving access to extremely large modulation bandwidths.[4–6]

Recently, using a lumped-element approach, we have reported the amplitude modulation up to 13 GHz of a 3 mm-long, metal-metal waveguide 2.8 THz QCL.[4] In order to further extend the radio frequency (RF)-modulation capabilities of THz QCLs, a more accurate approach to better quantify the amount of microwave power injected in the devices must now be considered. THz meta-metal waveguides (MMWs) are good candidates for high frequency RF-modulation.[4,7] In fact, as shown in Figs. 1(b) and 1(c) their topology is very similar to that of microwave thin-film, microstrip transmission lines, where an insulating, semi-infinite dielectric, is sandwiched between a ground plane and a top metallic stripe.[8] Still there are two important differences: the first arises from the fact that in a THz QCL MMW the dielectric consists of a *doped* $GaAs/Al_xGa_{1-x}As$ heterostructure, and the second from the fact that the latter is etched away on both sides of the top contact to form a ridge [see Fig. 1(b)]. Both these features are essential for the operation of these electrically pumped semiconductor lasers in order to (i) guarantee a sufficiently high vertical conductivity, and to (ii) avoid lateral spreading of the current. At the same time they have an important impact of the microwave attenuation and propagation, thus determining the modulation properties of THz QCLs. In this work, we have addressed this issue by measuring the transmission and reflection coefficients in the microwave range (S-parameters) of MMW THz QCLs emitting at 2.3 THz.

The devices used in this work are based on the $GaAs/Al_{0.2}Ga_{0.8}As$ active region presented in Ref. 9, and have an emission frequency of 2.3 THz. The active region is sandwiched between 80 and 600 nm-thick top and bottom GaAs contact layers, *n*-doped at levels of 5×10^{18} and 2×10^{18} cm^{-3}. The average doping level of the active region is 3×10^{15} cm^{-3}. MMWs were fabricated following the technique used in Ref. 10 (see Fig. 1 for dimensions). 16 μm thick and 61 μm wide ridges were cleaved into laser bars up to 4 mm-long and In-soldered onto copper holders screwed on the cold head of a continuous-flow He cryostat. For all the measurements in this work, the QCLs were operated in continuous wave at a heat sink temperature of 4 K.

In Fig. 2 we report representative experimental $(1-|S_{11}|^2)$ plots in the 0.1–55 GHz range for a 2.65 mm-long (top panel) and a 1 mm-long ridge (bottom panel). Measurements were performed at 4 K with the help of a vectorial network analyzer (Agilent PNA E8361A) coupled to a 50 Ω coplanar probe that was positioned at one end of the ridge with the other end left open-ended [see the schematic in Fig. 1(a)]. The analyzer was calibrated, thanks to alumina coplanar standards placed close to the samples. The lasers were first operated at current densities of 140 and 120 A/cm^2,

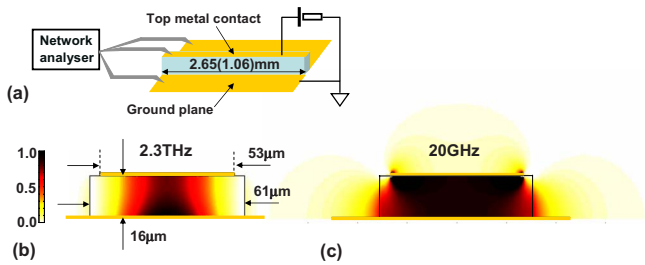

FIG. 1. (Color online) (a) Schematic of the experimental setup where a 50 Ω coplanar probe connected to a network analyzer is positioned over the THz QCL contacts. The QCL is 2.65 (1.06) mm-long and is driven at 4 K. [(b) and (c)] computed two-dimensional mode intensity profiles $|E_z(x,y)|^2$ along the section of the waveguide at 2.3 THz (b) and 20 GHz (c). E_z is the *z*-component of the electric field, and the *xy*-plane is the plane of the laser facet. The light orange horizontal lines represent the top metal contact and the ground plane.

a)Author to whom correspondence should be addressed. Electronic mail: stefano.barbieri@univ-paris-diderot.fr.

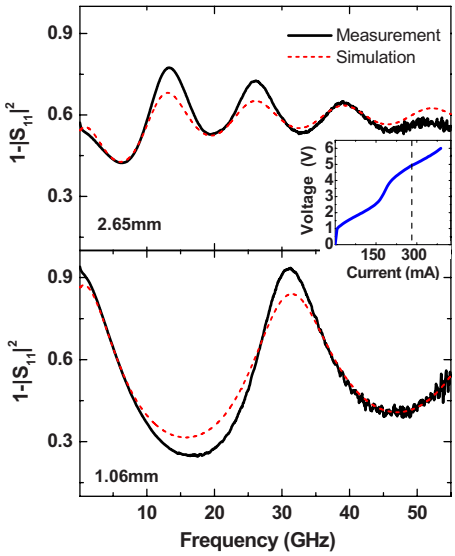

FIG. 2. (Color online) Measured (black solid line) and simulated (red dashed line) $(1-|S_{11}|^2)$ plots in the 0.1–55 GHz range for a 2.65 mm-long (top panel) and a 1.06 mm-long (bottom panel) ridge, driven at current densities of 140 and 120 A/cm^2 respectively. Inset: Voltage/current characteristic of the 2.65 mm-long ridge at 4 K. The vertical dashed line indicates the laser threshold (270 mA→160 A/cm^2).

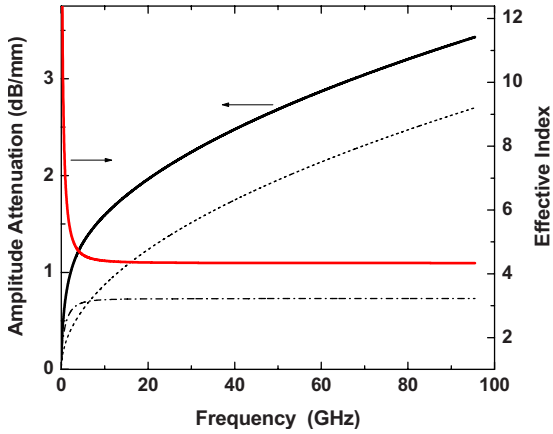

FIG. 3. (Color online) Microwave attenuation (black curve, left axis) and effective index (red curve, right axis) derived from the distributed parameters. As shown by the dashed lines the attenuation is given by the sum of two contributions: (i) a virtually frequency independent component due to the shunt conductance (dashed-dotted line) and (ii) a $\sqrt{f}$-dependent contribution stemming from the series resistance (dotted line).

respectively, i.e., just below the threshold for lasing, of 160 A/cm^2. Pronounced oscillations corresponding to the QCL cavity Fabry–Perot (FP) resonances are clearly visible, up to the fourth order for the 2.65 mm ridge and up to the first order for the 1 mm-long one. These oscillations are a consequence of the fact that the QCL is mismatched at each end, its characteristic impedance being different from 50 Ω. The decrease in the oscillation amplitude with increasing frequency indicates the presence of attenuation. To estimate the value of this attenuation we have fitted the experimental curves using a transmission line model, where the shunt conductance per unit length, $G=3\times10^{-2}$ S/mm, is obtained by dividing the experimental differential conductance of the devices at the operating point by the device length. For the series resistance per unit length we assumed a $\sqrt{f}$-dependence, where f is the microwave frequency.[8] This leads to a $\sqrt{f}$-dependence of the attenuation coefficient, which is consistent with the low frequency limit of free-carrier absorption derived from the Drude conductivity.[11] The dashed lines in Fig. 2 represent the obtained curves, from which we extract the following distributed parameters: $L=1.6\times10^{-10}$ H/mm, $C=1.3\times10^{-12}$ F/mm, and $R=4.5\times10^{-5}\sqrt{f}$ Ω/mm.[12]

In Fig. 3, we report the microwave attenuation (left axis) and the effective index (right axis) derived from the distributed parameters. As shown by the dashed lines the attenuation is the sum of the following two contributions: (i) a virtually frequency independent component due to the shunt conductance (dotted-dashed line) and (ii) a $\sqrt{f}$-dependent contribution stemming from the series resistance (dotted line). We note that at 50 GHz the latter is approximately 15 times higher than the surface resistance of Au at 4 K computed by taking into account the anomalous skin effect.[13] This shows that in our structure the attenuation is dominated by absorption in the contact layers and in the lightly doped QCL active region rather than in the metal contacts. In this respect, we note that the discrepancies in the oscillations amplitudes of Fig. 2 between the data and the fit, could be the result of deviations from the $\sqrt{f}$ dependence of the classical Drude conductivity due to low temperature localization into the donor states of the heavily doped contact layers. By defining the 3 dB modulation cutoff as the frequency at which the modulating voltage integrated over the total device length has dropped by a factor $1/\sqrt{2}$, from Fig. 3 we obtain 3 dB bandwidths of ~4 and 70 GHz for the 2.65 and 1.06 mm-long ridges, respectively. The latter is approximately equal to the intrinsic 3 dB cutoff of the QCL active region, that we estimated using a two-level rate equation model with an emitted power in the 0.5–1 mW range.[4,6]

We have taken advantage from the knowledge of the impedance of the QCL to realize high-frequency, narrow-band matchings at ~19 and 24 GHz, i.e., close to the high frequency limit of our microwave circuit. These were obtained by mounting the lasers at the end of a 50 Ω microstrip-line in parallel to a shunt open-stub.[8] In Fig. 4, we report the results of the 19 GHz matching, yielding intense modulation sidebands in the emission spectra of a single-mode, 4 mm-long, 2.3 THz QCL modulated between 18 and 21.5 GHz, using 13 dBm of microwave power from an RF generator (see the caption of Fig. 4 for experimental details). The inset shows the spectra resulting from the 24 GHz matching applied to a 1.5 mm-long, single mode lase. Sidebands are clearly visible between 24 and 24.7 GHz, the highest modulation frequencies reported to date for a QCL. In this case 20 dBm of microwave power were needed since we are close the high-frequency end of our microwave apparatus (cables and connectors).

In Fig. 5, two $(1-|S_{11}|^2)$ plots for the 2.65 mm device of Fig. 2 (top panel) are reported below and above the laser threshold. Above threshold we observe the presence of pronounced sharp peaks in correspondence to the maxima of the microwave FP resonances.[15] To investigate their origin we have recorded several THz emission spectra of the QCL above threshold with a Fourier transform spectrometer, as well as RF spectra of the bias voltage across the device with the help of a microwave spectrum analyzer. Both spectra (not shown) confirmed that the peaks of Fig. 5 result from the beating of the longitudinal THz FP modes of the QCL.[16] To a first approximation these are separated by multiples of the cavity THz round-trip frequency, $f_{RT}^{THz}=(2n_G^{THz}L)^{-1}(\mathrm{cm}^{-1})$,

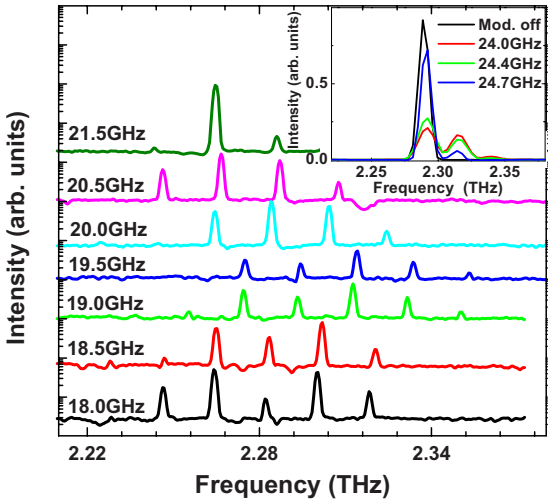

FIG. 4. (Color online) Spectra in Log_{10} scale from a 4 mm-long, 2.3 THz, MMW QCL, amplitude modulated at frequencies between 18 and 21.5 GHz, with an RF power of 13 dBm. Without modulation the QCL is single mode. The THz spectra were up-converted at 1.55 μm and measured with a high resolution optical spectrum analyzer using the technique described in Refs. 4 and 14. Inset: Spectra in linear scale of a 1.5 mm-long, 2.3 THz, MMW QCL, amplitude modulated at frequencies between 24.0 and 24.7 GHz, with an RF power of 20 dBm. Spectra were collected with a Fourier transform spectrometer with a resolution of 0.25 cm^{-1}.

where n_G^{THz} is the THz group effective index and L the cavity length. The fact that f_{RT}^{THz} is coincident with the maxima of the microwave FP oscillations positioned at multiples of $f_{FP}^{\mathrm{GHz}}=(2n_{\mathrm{eff}}^{\mathrm{GHz}}L)^{-1}(\mathrm{cm}^{-1})$, where $n_{\mathrm{eff}}^{\mathrm{GHz}}$ is the effective index of the gigahertz (GHz) mode, is not trivial. We believe that this is the result of two effects. On the one hand, a self seeding effect is present that pulls the roundtrip frequency of the QCL in proximity of the microwave FP resonance peaks even without external RF power.[17] On the other hand $n_G^{\mathrm{THz}} \cong n_{\mathrm{eff}}^{\mathrm{GHz}}$, i.e., the microwave is propagating at a speed that is close to that of the THz envelope. To investigate this hypothesis, in the Inset of Fig. 5 (blue line) we report the computed group effective index at 2.3 THz as a function of ridge width using a home-made finite difference code developed by us. The refractive index of the doped GaAs layers was computed using the Drude conductivity, with $\varepsilon_\infty=13.3$ and a scattering time in the range 0.1–1 ps.[11] The red line in the inset reports

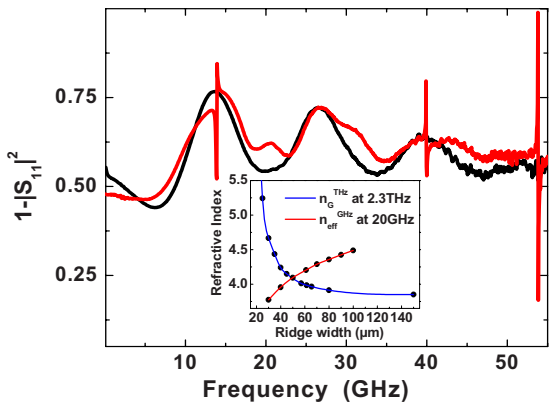

FIG. 5. (Color online) Measured $(1-|S_{11}|^2)$ plots in the 0.1–55 GHz range for the 2.65 mm-long device at current densities of 250 mA (below threshold) and 330 mA (above threshold), respectively. Inset: Computed group effective index at 2.3 THz (n_G^{THz}, blue line) and effective index at 20 GHz ($n_{\mathrm{eff}}^{\mathrm{GHz}}$, red line) as a function of the ridge width.

instead the microwave effective index computed using a commercial code (COMSOL Multiphysics®) at $f=20$ GHz. Here the choice of ε_∞ for doped GaAs is much more critical as the literature provides very sparse experimental values.[18] Moreover, the latter is heavily dependent on the choice of the scattering time since f is much smaller than the plasma frequency. We have therefore adopted the phenomenological approach of introducing an effective bulk permittivity of 25, giving the experimental value of $n_{\mathrm{eff}}^{\mathrm{GHz}}$ derived from the positions of the FP resonance maxima of Fig. 5 ($n_{\mathrm{eff}}^{\mathrm{GHz}} \approx 4.3$, see also Fig. 3).[19] As shown in the Inset of Fig. 5 the n_G^{THz} and $n_{\mathrm{eff}}^{\mathrm{GHz}}$ curves have opposite slopes and intersect for a ridge width of ~ 50 μm, corresponding to $n_G^{\mathrm{THz}}=n_{\mathrm{eff}}^{\mathrm{GHz}} \cong 4.1$, which is 5% off with respect the experimental value of $n_G^{\mathrm{THz}} \cong 4.3$. We believe that this discrepancy is within the precision of our modeling and experimental data; what must be retained here, is that the condition $n_G^{\mathrm{THz}}=n_{\mathrm{eff}}^{\mathrm{GHz}}$ is effectively determined by the width of the ridge. Although not directly relevant for the modulation bandwidth of THz QCLs, this THz-GHz "phase matching" could be exploited for the realization of THz traveling-wave modulators.[20]

Paul Crozat, Daniel Dolfi, and Jerome Faist are gratefully acknowledged for helpful discussions. We thank S. Lepillet and the Characterization Center of IEMN for technical assistance. Partial financial support from the Délégation Générale pour l'Armement (Contract No. 06.34.020) and the initiative C-Nano Ile-de-France TeraCascadeare also acknowledged.

[1] W. Chan, H. Chen, A. Taylor, I. Brener, M. Cich, and D. Mittleman, Appl. Phys. Lett. **94**, 213511 (2009).
[2] H. Chen, W. Padilla, M. Cich, A. Azad, R. Averitt, and A. Taylor, Nat. Photonics **3**, 148 (2009).
[3] P. Kužel, F. Kadlec, J. Petzelt, J. Schubert, and G. Panaitov, Appl. Phys. Lett. **91**, 232911 (2007).
[4] S. Barbieri, W. Maineult, S. S. Dhillon, C. Sirtori, J. Alton, and N. Breuil, Appl. Phys. Lett. **91**, 143510 (2007).
[5] B. S. Williams, Nat. Photonics **1**, 517 (2007).
[6] R. Paiella, R. Martini, F. Capasso, C. Gmachl, H. Y. Hwang, D. L. Sivco, J. N. Ballargeon, A. Y. Cho, E. A. Whyttaker, and H. C. Liu, Appl. Phys. Lett. **79**, 2526 (2001).
[7] S. Kohen, B. S. Williams, and Q. Hu, J. Appl. Phys. **97**, 053106 (2005).
[8] S. Ramo, J. R. Whinnery, and T. V. Duzer, *Field and Waves in Communication Electronics*, 2nd ed. (Wiley, New York, 1984).
[9] C. Worrall, J. Alton, M. Houghton, S. Barbieri, H. E. Beere, D. A. Ritchie, and C. Sirtori, Opt. Express **14**, 171 (2006).
[10] S. S. Dhillon, J. Alton, S. Barbieri, C. Sirtori, A. De Rossi, M. Calligaro, H. E. Beere, and D. A. Ritchie, Appl. Phys. Lett. **87**, 071107 (2005).
[11] P. Y. Yu and M. Cardona, *Fundamentals of Semiconductors* (Springer, Berlin, 1996).
[12] With the same distributed parameters; we obtain a good agreement also with the S_{12} experimental curves (not shown).
[13] L. W. Duncan, IEEE Trans. Microwave Theory Tech. **19**, 130 (1968).
[14] S. Dhillon, C. Sirtori, J. Alton, S. Barbieri, A. De Rossi, H. Beere, and D. Ritchie, Nat. Photonics **1**, 411 (2007).
[15] Further measurements are under way to understand the origin of the additional wide peaks at $\sim$20 and 30 GHz.
[16] S. Barbieri, J. Alton, C. Baker, T. Lo, H. Beere, and D. Ritchie, Opt. Express **13**, 6497 (2005).
[17] That the number of FP modes increases when the RF modulation frequency is tuned close to the THz QCL cavity round trip was shown in Ref. 4.
[18] N. Katzenellenbogen and D. Grischkowsky, Appl. Phys. Lett. **61**, 840 (1992).
[19] The metal contacts were approximated as perfect conductors.
[20] J.-M. Liu, *Photonic Devices* (Cambridge University Press, Cambridge, 2005).